

Petrological evidence for secular cooling in mantle plumes

Claude Herzberg¹ & Esteban Gazel¹

Geological mapping and geochronological studies have shown much lower eruption rates for ocean island basalts (OIBs) in comparison with those of lavas from large igneous provinces (LIPs) such as oceanic plateaux and continental flood provinces¹. However, a quantitative petrological comparison has never been made between mantle source temperature and the extent of melting for OIB and LIP sources. Here we show that the MgO and FeO contents of Galapagos-related lavas and their primary magmas have decreased since the Cretaceous period. From petrological modelling², we infer that these changes reflect a cooling of the Galapagos mantle plume from a potential temperature of 1,560–1,620 °C in the Cretaceous to 1,500 °C at present. Iceland also exhibits secular cooling, in agreement with previous studies^{3,4}. Our work provides quantitative petrological evidence that, in general, mantle plumes for LIPs with Palaeocene–Permian ages were hotter and melted more extensively than plumes of more modern ocean islands. We interpret this to reflect episodic flow from lower-mantle domains that are lithologically and geochemically heterogeneous.

Extensive outcrops of basalt, picrite, and sometimes komatiite ~65–95 Myr old occupy portions of the Caribbean LIP (CLIP). It has been suggested⁵ that they were produced by melting in the Galapagos mantle plume, and this is consistent with isotopic and geochemical similarities with lavas from the present-day Galapagos hotspot⁶. A Galapagos link for rocks in South American oceanic complexes is more controversial. Basalts, picrites, and komatiites from Gorgona Island, Columbia, were originally considered part of the CLIP^{7,8}. However, other studies⁹ suggest Gorgona and other South American complexes were once part of a separate oceanic plateau related to Salas y Gomez Island, Chile, or some other hotspot (Supplementary Information).

The lowest FeO contents are mostly found in lavas 0–13 Myr old from the present-day Galapagos archipelago and the Carnegie ridge and Cocos ridge hotspot tracks (Fig. 1a). FeO contents are highest for Gorgona komatiites and intermediate for all other lavas. When olivine is the sole crystallizing phase, lavas with higher FeO contents can be differentiated from peridotite-source primary magmas with higher FeO and MgO contents^{2,3,10–12} (Fig. 1a). A primary magma is a partial melt of the mantle formed, in most cases, by the mixing of small melt droplets that are separated from the remainder of the solid residue^{2,3,10,11}. Addition or subtraction of olivine from a primary magma will produce lavas having higher or lower MgO contents, respectively, with minor change in FeO content. We simulated this and reconstructed the primary magma compositions using the PRIMELT2 model of ref. 2 (Methods Summary). Our results are given in Supplementary Information and Fig. 1a.

The MgO content of a volatile-deficient primary magma is positively correlated with the temperature of the mantle^{2,3,10–12}. It provides a petrological record of mantle potential temperature, T_p , which is the temperature that the solid adiabatically convecting mantle would

attain if it could reach the surface without melting¹³. Using the relationship $T_p = 1,463 + 12.74\text{MgO} - 2,924/\text{MgO}$ (refs 2, 3; here MgO is measured in weight per cent and T_p is given in degrees Celsius), we can now readily calculate how hot the mantle had to be to yield the primary magma compositions given in Fig. 1a. Our results are shown in Figs 1b and 2. For the present-day Galapagos plume, T_p ranges from 1,400 to 1,500 °C (ref. 2), similar to the T_p range of 1,440–1,500 °C recorded for lavas from the Cocos and Carnegie ridges. Older lavas were hotter. Those from the CLIP and accreted tracks with ages of 65–95 Myr have a T_p range of 1,500 to 1,560 °C, and up to 1,620 °C if Gorgona lavas were part of the CLIP. This is petrological evidence for secular cooling of the Galapagos plume.

The MgO content of an accumulated fractional melt does not change substantially as melt fraction increases during decompression^{2,3,11}. The adiabatic temperature–pressure melting path is approximately coincident with the olivine liquidus, which can be calculated using $T_{OL} = 935 + 33\text{MgO} - 0.37(\text{MgO})^2 + 54P - 2P^2$, where T_{OL} and MgO are measured as above and pressure, P , is measured in gigapascals^{2,11}. Using final melting pressures and the MgO contents of primary magmas in this equation (Fig. 1a), a synthetic adiabatic melting path can be obtained (Fig. 1b). The majority of lavas from the present-day Galapagos plume formed in a column where melting ended at >2 GPa, and this pressure is highly variable. Melting ended at much lower pressures for lavas from the Cocos and Carnegie ridges, consistent with the channelling of the Galapagos plume to locations of thinner lithosphere. Low pressures of final melting are also inferred for many older CLIP lavas, indicating the possible involvement of thin lithosphere associated with ocean ridges.

We now provide petrological evidence for secular cooling in other areas. Results given in Supplementary Information and Fig. 2 illustrate that LIPs dating from the Palaeocene epoch and earlier were formed by mantle sources that were generally hotter than present-day ocean islands. However, there are several important exceptions. First, Hawaii is the ocean island that is most similar to a LIP, in that it has a maximum T_p of 1,600 °C. It is only surpassed by rocks from the North Atlantic igneous province, the Deccan Traps and the CLIP if we include Gorgona. Second, T_p for the Central Atlantic magmatic province (CAMP) is notably different from all other LIPs in being cool (Fig. 2). The T_p excess of ~100 °C for the CAMP is consistent with model temperatures¹⁴ that can arise from an internally heated mantle capped by Pangaea^{14,15}. This is evidence indicating that continental insulation is not capable of producing LIPs with the much higher values of T_p (Fig. 2).

Noteworthy is the wide range of primary magma compositions and inferred mantle potential temperatures for each LIP and ocean island occurrence (Fig. 2). These ranges have been interpreted as originating from a hotspot, a spatially localized source of heat and magmatism restricted in time². Primary magmas are tapped from both the hot axis and the cool periphery of the plume as illustrated

¹Department of Earth and Planetary Sciences, Rutgers University, 610 Taylor Road, Piscataway, New Jersey 08854-8066, USA.

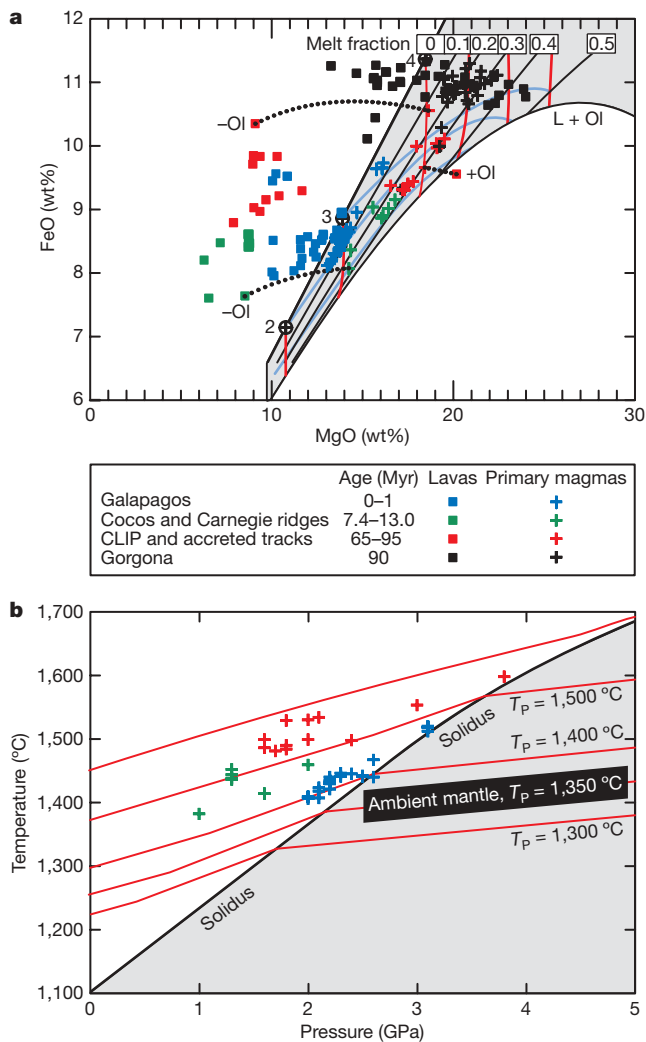


Figure 1 | Compositions and inferred temperature–pressure conditions of melting for Galapagos-related magmatism. **a**, FeO and MgO contents of lavas and calculated primary magmas from the present-day Galapagos hotspot, the Cocos and Carnegie ridges, old accreted Galapagos tracks and the CLIP. Lavas from Gorgona are plotted separately because it is not clear whether they were part of the CLIP^{7,8} or some other oceanic complex⁹. Lines of filled circles identify liquid compositions that result from olivine addition to (+) and subtraction from (–) specific lava compositions. Primary magma compositions were computed using PRIMELT2². Primary magmas of fertile peridotite KR-4003 are plotted within the grey-coloured area². The intersection of a red line (initial melting pressure) and a blue line (final melting pressure) identifies the composition of an accumulated fractional melt at the pressure of initial and final melting. Individual lavas and their sources from which primary magmas are calculated are identified in Supplementary Table 1. Pressure is indicated in gigapascals by the circled crosses, as shown. L, liquid; Ol, olivine. **b**, Inferred temperatures and pressures at which fractional melting terminated (Methods). Red lines, adiabatic melting paths¹¹. Gorgona komatiites probably formed from a more depleted peridotite source³, and solutions are not provided.

in Fig. 3. The T_P maximum of $1,500\text{ }^\circ\text{C}$ for Galapagos is characteristic of the plume axis. The lower end of the Galapagos range approaches $1,350 \pm 50\text{ }^\circ\text{C}$, a T_P value for ambient mantle^{3,10,16,17} necessary for the production of MORB with 10–13 wt% MgO. What is particularly relevant for our purposes is that there is a decrease in T_P maxima from $1,560\text{--}1,620\text{ }^\circ\text{C}$ for rocks 65–95 Myr old to $1,500\text{ }^\circ\text{C}$ at present (Fig. 2). The exact form of the secular cooling curve depends on whether the Gorgona komatiites were produced by the Galapagos plume or another (Supplementary Information).

Melt fractions computed from PRIMELT2 are generally higher for LIPs than for ocean islands (Fig. 4), consistent with suggestions of

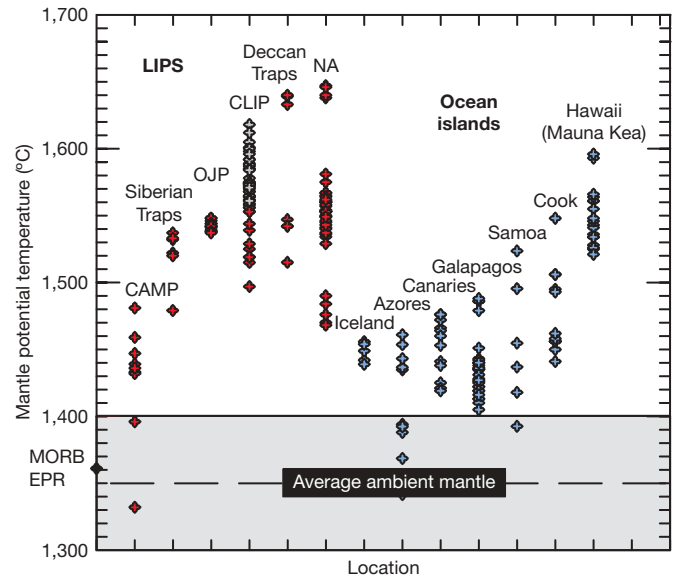


Figure 2 | Mantle potential temperatures inferred for lavas from some LIPs and ocean islands. T_P has been computed from primary magma MgO content using PRIMELT2². Data sources and calculated T_P values for ocean islands and LIPs are given in Supplementary Information. CLIP results are for rocks with ages ≥ 65 Myr, and include old accreted Galapagos tracks. Gorgona data is shown separately using grey crosses. Galapagos results are from lavas within the archipelago. OJP, primary magmas for lavas from the Ontong Java plateau; NA, primary magmas for Palaeocene lavas from the North Atlantic igneous province found in East and West Greenland; CAMP, primary magmas for the Central Atlantic magmatic province; MORB, mid-ocean-ridge basalt; EPR, East Pacific Rise.

higher eruption rates¹. The high melt fractions, high mantle potential temperatures and vast areas of magmatism associated with the largest LIPs are all consistent with formation in mantle plume heads¹ (but note the possible CAMP exception). By contrast with LIPs, many ocean islands display melt fractions that must be lower than ~ 0.05 (Fig. 4b). These are often readily characterized by very low SiO_2 , high CaO and high lithophile trace-element abundances in OIBs owing to low-degree melting of carbonated peridotite^{2,18}. Low-melt-fraction, CO_2 -rich OIBs are abundant in the Azores, the Canary Islands, Cape Verde, the Cook–Austral chain, the Marquesas Islands, the Pitcairn–Gambier chain, St Helena, Samoa and the Society Islands, and many other ocean islands (see, for example, the *Geochemistry of Rocks of the Oceans and Continents* database (<http://georoc.mpch-mainz.gwdg.de/georoc/>) and Supplementary Information). Even more of this OIB-type melt is likely to metasomatize the mantle rather than erupt. The melt-fraction frequency spectrum for OIB in Fig. 4b is

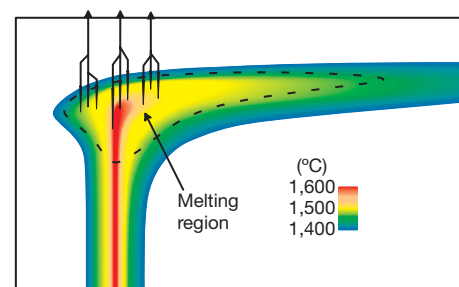


Figure 3 | A generic model for interpreting the spatial localization of petrological variability. The model provides an interpretation of primary magmas with highly variable compositions, inferred mantle potential temperatures and melt fractions. This is the mantle plume model in which hot primary magmas originate from the axis and cooler primary magmas originate from the periphery. The colour bar indicates mantle potential temperature.

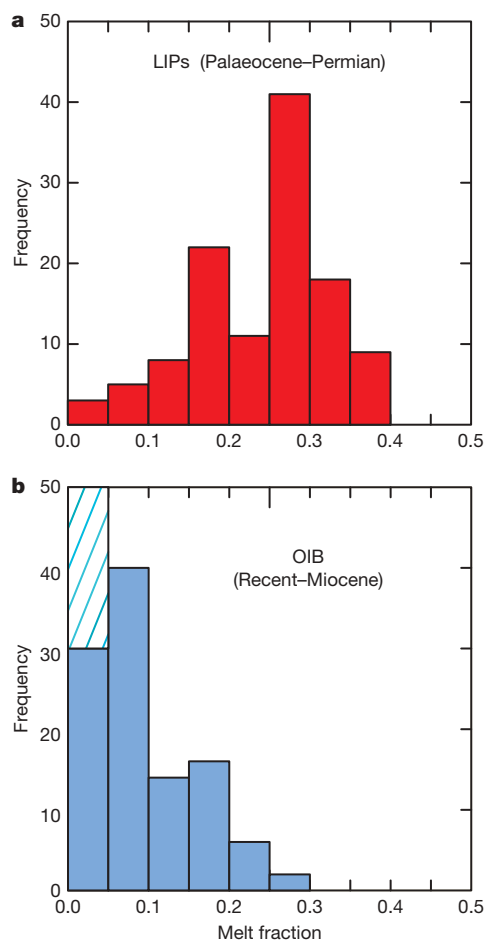


Figure 4 | Melt fractions inferred for lavas for some LIPs and ocean islands.

Melt fractions have been computed using PRIMELT2², and refer to the total melt fraction with respect to source mass for accumulated fractional melting of fertile peridotite. **a**, LIPs. Data sources for model primary magmas for LIPs are given in Supplementary Information. **b**, OIB. Solid blue bars indicate primary magma solutions from ocean islands (see ref. 2 and Supplementary Information). The hatched region indicates an abundance of OIB melted from volatile-enriched sources at very low melt fractions; these are generally more abundant than volatile-deficient lavas, and cannot be modelled with PRIMELT2 (see fig. 11 in ref. 2). Frequency is the number of primary magma solutions.

therefore likely to be exponential in form. Results for these OIB occurrences are interpreted as the transport of low-melt-fraction magmas from the cool plume peripheries and high-melt-fraction magmas from the hotter plume axes (Fig. 3). However, it has been proposed that low-melt-fraction OIB can also form without a plume by volatile-induced melting of ambient mantle and transport through lithospheric fractures¹⁹. This suggestion is fully consistent with experiments¹⁸ and PRIMELT2² modelling. Both plume and non-plume origins are indicated for ocean islands.

A very high cooling rate is inferred for the Icelandic plume. Most Palaeocene lavas with ~60-Myr pre-breakup ages²⁰ from East and West Greenland have T_p maxima of ~1,550–1,570 °C, similar to the CLIP, and crystallized from primary magmas with 18–20 wt% MgO. Our model primary magmas are in excellent agreement with many previous estimates^{3,4,11,21}, although we obtained T_p values as high as 1,650 °C (Fig. 2). A spread of ~200 °C in T_p and melt fractions in the range 0.05–0.37 have been recorded in East Greenland lavas (Supplementary Information) from a restricted area close to the Tertiary Icelandic hotspot track²². These ranges are an expected consequence of the tapping of primary magmas from a mantle plume (Fig. 3). A T_p value as low as 1,460 °C has been obtained from lavas with ~55-Myr syn-breakup ages from the seaward-dipping reflector

sequence, similar to present-day Iceland^{2,3,23} (Fig. 2). Our work indicates that T_p decreased from the range 1,550–1,650 °C to 1,460 °C in about 5 Myr, in agreement with estimates in ref. 4. The T_p value for the Icelandic plume appears unchanged at about 1,460 °C from 55 Myr ago to the present, and is now in a comparatively steady state. The early rapid secular cooling of the Icelandic plume is much greater than that seen for the Galapagos, although more work is needed to fill the gap in the Galapagos data (Supplementary Information). We also acknowledge that an Icelandic plume cooling curve is compromised by an absence of data from the Greenland–Iceland and Iceland–Faeroes ridges with ~15–50-Myr ages.

Our work provides petrological evidence that mantle plumes for LIPs with Palaeocene–Permian ages were hotter and melted more extensively than plumes of more modern ocean islands. One interpretation is that LIPs melted from large plume heads and OIBs melted from thin plume conduits¹, and cooling is more effective in the latter. Indeed, there is now an important literature on lithosphere and asthenosphere cooling of mantle plumes^{24,25}. However, this explanation fails to explain why hot LIPs such as those in Fig. 2 are not erupting today.

Numerical and laboratory simulations show that mantle flow can be episodic where there are thermal and compositional components to buoyancy^{25–27}. Mantle plumes with these characteristics might originate in lower-mantle domains where shear-wave velocities are low and bulk density is intrinsically high^{28,29}. Subduction can contribute to high silica content³⁰, and iron content that is both high³⁰ and low in these domains (Methods), and mixing may yield heterogeneities on a range of length scales. Plumes may randomly sample this complexity, or lighter components may preferentially separate from more dense lithologies that stay behind. Although progress is being made on identifying peridotite and subducted crustal source lithologies from the compositions of lavas, inferring iron content is a much more difficult problem (Methods). Nevertheless, we are optimistic that integrated petrological and deep-mantle studies can provide a better picture of the birth–life–death cycle of mantle plumes.

METHODS SUMMARY

Primary magma compositions, mantle potential temperatures and source melt fractions were calculated from primitive whole-rock compositions using PRIMELT2 spreadsheet software². A detailed discussion of the method is given elsewhere^{2,3,11}. The algorithm calculates the primary magma composition for a primitive lava by determining the variable amounts of olivine that were added or subtracted.

PRIMELT2 was calibrated on the basis of experiments on fertile peridotite with 8 wt% FeO, and all calculated primary magma compositions were assumed to have been derived by fractional melting. For each primary magma, it provided the olivine liquidus temperature, T_{OL} , at 1 atm and the mantle potential temperature, T_p . As both T_{OL} and T_p depend on the MgO content of the primary magma³, the accuracy of the former is a guide to the precision of the latter. For any specific peridotite composition, the uncertainty in T_{OL} is ± 31 °C at the 2σ confidence level³. Uncertainties in the FeO content of peridotite can propagate to an uncertainty of ± 50 –70 °C in T_p (Methods). Uncertainties in all other major elements for fertile peridotite do not propagate to significant variations in melt fraction and mantle potential temperature^{2,11}. Melting of depleted peridotite propagates to calculated melt fractions that are too high, but with a negligible error in mantle potential temperature^{2,3,11}.

We used PRIMELT2 to identify magmas generated from pyroxenite sources, and excluded them. Magmas that have been degassed from CO₂-rich sources were identified and similarly excluded. Fe₂O₃ content was calculated using Fe₂O₃/TiO₂ = 0.5, a reduced mode, on the basis of MORB-like FeO enrichment for most LIPs². Lavas that had experienced plagioclase and/or clinopyroxene fractionation were excluded from this analysis.

Full Methods and any associated references are available in the online version of the paper at www.nature.com/nature.

Received 4 September 2008; accepted 28 January 2009.

- Richards, M. A., Duncan, R. A. & Courtillot, V. E. Flood basalts and hot-spot tracks: plume heads and tails. *Science* **246**, 103–107 (1989).
- Herzberg, C. & Asimow, P. D. Petrology of some oceanic island basalts: PRIMELT2.XLS software for primary magma calculation. *Geochem. Geophys. Geosyst.* **9**, doi:10.1029/2008GC002057 (2008).

3. Herzberg, C. *et al.* Temperatures in ambient mantle and plumes: constraints from basalts, picrites and komatiites. *Geochem. Geophys. Geosyst.* **8**, doi:10.1029/GC001390 (2007).
4. Armitage, J. J., Henstock, T. J., Minshull, T. A. & Hopper, J. R. Modelling the composition of melts formed during continental breakup of the Southeast Greenland margin. *Earth Planet. Sci. Lett.* **269**, 248–258 (2008).
5. Duncan, R. A. & Hargraves, R. B. Plate tectonic evolution of the Caribbean region in the mantle reference frame. *Bull. Geol. Soc. Am.* **162**, 81–93 (1984).
6. Hoernle, K., Hauff, F. & van den Bogaard, P. 70 m.y. history (139–69 Ma) for the Caribbean large igneous province. *Geology* **32**, 697–700 (2004).
7. Storey, M., Mahoney, J. J., Kroenke, L. W. & Saunders, A. D. Are oceanic plateau sites for komatiite formation? *Geology* **19**, 376–379 (1991).
8. Kerr, A. C. *et al.* The petrogenesis of Gorgona komatiites, picrites and basalts: new field, petrographic and geochemical constraints. *Lithos* **37**, 245–260 (1996).
9. Kerr, A. C. & Tarney, J. Tectonic evolution of the Caribbean and northwestern South America: The case for accretion of two Late Cretaceous oceanic plateaus. *Geology* **33**, 269–272 (2005).
10. Langmuir, C. H., Klein, E. M. & Plank, T. in *Mantle Flow and Melt Generation at Mid-Ocean Ridges* (eds Morgan, J. P., Blackman, D. K. & Sinton, J. M.) 183–280 (Geophys. Monogr. Ser. 71, American Geophysical Union, 1992).
11. Herzberg, C. & O'Hara, M. J. Plume-associated ultramafic magmas of Phanerozoic age. *J. Petrol.* **43**, 1857–1883 (2002).
12. Putirka, K. D. Mantle potential temperatures at Hawaii, Iceland, and the mid-ocean ridge system, as inferred from olivine phenocrysts: evidence for thermally driven mantle plumes. *Geochem. Geophys. Geosyst.* **6**, doi:10.1029/2005GC000915 (2005).
13. McKenzie, D. & Bickle, M. J. The volume and composition of melt generated by extension of the lithosphere. *J. Petrol.* **29**, 625–679 (1988).
14. Coltice, N., Phillips, B. R., Bertrand, H., Richard, Y. & Rey, P. Global warming of the mantle at the origin of flood basalts over supercontinents. *Geology* **35**, 391–394 (2007).
15. Anderson, D. L. Hotspots, polar wander, Mesozoic convection and the geoid. *Nature* **297**, 391–393 (1982).
16. McKenzie, D., Jackson, J. & Priestley, K. Thermal structure of oceanic and continental lithosphere. *Earth Planet. Sci. Lett.* **233**, 337–349 (2005).
17. Courtier, A. M. *et al.* Correlation of seismic and petrological thermometers suggests deep thermal anomalies beneath hotspots. *Earth Planet. Sci. Lett.* **264**, 308–316 (2007).
18. Dasgupta, R., Hirschmann, M. M. & Smith, N. D. Partial melting experiments on peridotite + CO₂ at 3 GPa and genesis of alkalic ocean island basalts. *J. Petrol.* **48**, 2093–2124 (2007).
19. Hirano, N. *et al.* Volcanism in response to plate flexure. *Science* **313**, 1426–1428 (2006).
20. Storey, M., Ducan, R. A. & Tegner, C. Timing and duration of volcanism in the North Atlantic igneous province: implications for geodynamics and links to the Iceland hotspot. *Chem. Geol.* **241**, 264–281 (2007).
21. Holm, P. M. *et al.* The tertiary picrites of West Greenland: contributions from 'Icelandic' and other sources. *Earth Planet. Sci. Lett.* **115**, 227–244 (1993).
22. Saunders, A. D., Fitton, J. G., Kerr, A. C., Norry, M. J. & Kent, R. W. in *Large Igneous Provinces: Continental, Oceanic, and Planetary Flood Volcanism* (eds Mahoney, J. J. & Coffin, M. J.) 45–93 (Geophys. Monogr. Ser. 100, American Geophysical Union, 1997).
23. Slater, L., McKenzie, D., Grönvold, K. & Shimizu, N. Melt generation and movement beneath Theistareykir, NE Iceland. *J. Petrol.* **42**, 321–354 (2001).
24. Sleep, N. Channeling at the base of the lithosphere during the lateral flow of plume material beneath flow line hot spots. *Geochem. Geophys. Geosyst.* **9**, doi:10.1029/2008GC002090 (2008).
25. Kumagai, I., Davaille, A., Kurita, K. & Stutzmann, E. Mantle plumes: thin, fat, successful, or failing? Constraints to explain hot spot volcanism through time and space. *Geophys. Res. Lett.* **35**, doi:10.1029/2005GL035079 (2008).
26. Farnetani, C. G. & Samuel, H. Beyond the thermal plume paradigm. *Geophys. Res. Lett.* **32**, doi:10.1029/2005GL022360 (2005).
27. Lin, S.-C. & van Keken, P. E. Multiple volcanic episodes of flood basalts caused by thermochemical mantle plumes. *Nature* **436**, 250–252 (2005).
28. Garnero, E. J. & McNamara, A. K. Structure and dynamics of Earth's lower mantle. *Science* **320**, 626–628 (2008).
29. Burke, K., Steinberger, B., Torsvik, T. H. & Smethurst, M. A. Plume generation zones at the margins of large low shear velocity provinces on the core–mantle boundary. *Earth Planet. Sci. Lett.* **265**, 49–60 (2008).
30. Trampert, J., Deschamps, F., Resovsky, J. & Yuen, D. Probabilistic tomography maps chemical heterogeneities throughout the lower mantle. *Science* **306**, 853–856 (2004).

Supplementary Information is linked to the online version of the paper at www.nature.com/nature.

Acknowledgements We are grateful to N. Sleep and A. Kerr for reviews, and to C. Class, M. Hirschmann, P. Asimow, M. Humayun and K. Hoernle for discussions.

Author Information Reprints and permissions information is available at www.nature.com/reprints. Correspondence and requests for materials should be addressed to C.H. (herzberg@rci.rutgers.edu).

METHODS

We assumed that all OIB and LIP lavas melted from peridotite with 8.0 wt% FeO, which is the average for natural fertile and depleted peridotite occurrences¹¹. We acknowledge, however, that mantle plume sources might differ if they originated in chemically unusual lower-mantle domains where shear-wave velocities are low and density is intrinsically high²⁸. These domains may contain subducted oceanic crustal rocks of Archaean and Proterozoic ages, which are iron-rich picrites³¹ and which might have reacted with host peridotite to produce a variety of iron-rich peridotite and pyroxenite lithologies as inferred from seismic and geodynamic data^{30,32}. Iron-rich crust would have left behind complementary iron-poor peridotite residues with FeO contents <8.0% (ref. 31); that which did not construct cratonic lithospheric mantle³¹ could have been subducted to yield lower-mantle domains that are low in FeO. There is likely to be substantial heterogeneity in iron on a scale that is too fine to be resolved using seismic data.

Progress has been made on identifying peridotite and pyroxenite source lithologies from the compositions of lavas^{33,34}, and this is encoded in PRIMELT2. However, inferring the iron content of a source from a lava composition is a much more difficult problem. If some OIB and LIPs melted from iron-rich peridotite with 9 wt% FeO, for example, model primary magmas will be too high in MgO^{2,11}, and the mantle potential temperatures summarized in Fig. 2 will be 50–70 °C too high. This is strictly an artefact of the computational method for primary magma calculation, and is not to be confused with higher mantle potential temperatures that are needed to make iron-rich mantle buoyant. Greater iron enrichment is not likely, as it would propagate to lava SiO₂ contents that are lower than observed, on the basis of experimental results of Kushiro³⁵. For iron-poor peridotite with 7 wt% FeO, potential temperatures will be too low by about 70 °C. There is little else we can do at present other than acknowledge the potential importance of iron variability in lower-mantle plume sources^{30,32}.

We have assumed that primary magmas are formed by accumulated fractional melting^{2,3,10,11}. The initial melting pressure, P_i , and final melting pressure, P_f , are indicated in Fig. 1a by the red and blue lines, respectively. These have been calculated by forward simulations of fractional melting of fertile peridotite^{11,31}. The final melting pressure is useful because it permits the construction of a synthetic temperature–pressure adiabatic melting path (Fig. 1b). The final melting pressure can be inferred by simply plotting FeO content and MgO content for a PRIMELT2 primary magma in Fig. 1a and interpolating using the blue lines. Alternatively, the final melting pressure can be calculated using the following equations. For primary magmas with <15 wt% MgO

$$P_{1f} = a + b\text{FeO} + c(\text{FeO})^2$$

Here FeO is the weight per cent of iron in the primary magma and a , b , and c are variables that depend on the MgO content of the primary magma:

$$a = -196.4 + 2.942\text{MgO} + 430/\text{MgO}$$

$$b = 17.7 - 0.444\text{MgO} + 228/\text{MgO}$$

$$c = 2.2 - 0.047\text{MgO} - 42.78/\text{MgO}$$

For primary magmas with 15% > MgO < 20%, the appropriate pressure to use is

$$P_{2f} = P_{1f} - 10.96 + 0.67\text{MgO}$$

The difference between calculated P_f values and those indicated in Fig. 1a by the blue lines is ± 0.28 GPa (2σ). Complex changes in phase equilibria will probably restrict pressure inferences for other OIB and LIP primary magmas to MgO < 20% and P_f < 3.5 GPa, similar to those for Galapagos and CLIP primary magmas.

Initial melting for garnet peridotite in the 2.7 GPa < P_i < 7 GPa range can be inferred by simply plotting FeO content and MgO content for a PRIMELT2 primary magma in Fig. 1a and interpolation using the red lines. Alternatively, they can be calculated from PRIMELT2 solutions for primary magma MgO contents using the equation

$$P_i = 11.248\text{MgO} - 13,700(1/\text{MgO})^3 - 8.13(\ln \text{MgO})^3$$

where the difference between calculated P_i values and those indicated in Fig. 1a by the red lines is ± 0.20 GPa (2σ).

31. Herzberg, C. Geodynamic information in peridotite petrology. *J. Petrol.* **45**, 2507–2530 (2004).
32. Forte, A. M. & Mitrovica, J. X. Deep-mantle high-viscosity flow and thermochemical structure inferred from seismic and geodynamic data. *Nature* **410**, 1049–1056 (2001).
33. Sobolev, A. V., Hofmann, A. W., Sobolev, S. V. & Nikogosian, I. K. An olivine-free mantle source of Hawaiian shield basalts. *Nature* **434**, 590–597 (2005).
34. Herzberg, C. Petrology and thermal structure of the Hawaiian plume from Mauna Kea volcano. *Nature* **444**, 605–609 (2006).
35. Kushiro, I. in *Earth Processes: Reading the Isotopic Code* (eds Basu, A. & Hart, S.) 109–122 (Geophys. Monogr. Ser. 95, American Geophysical Union, 1996).